Journal of Cosmology
and Astroparticle
Physics

PAPER • OPEN ACCESS

A low-redshift preference for an interacting dark energy model

To cite this article: Yuejia Zhai *et al* JCAP11(2025)010

Journal of Cosmology and Astroparticle Physics
An IOP and SISSA journal

Received: *April 4, 2025*
Revised: *September 23, 2025*
Accepted: *September 29, 2025*
Published: *November 5, 2025*

A low-redshift preference for an interacting dark energy model

Yuejia Zhai,[a] **Marco de Cesare**,[b,c] **Carsten van de Bruck**,[a]
Eleonora Di Valentino[a] **and Edward Wilson-Ewing**[d,e]

[a] *School of Mathematical and Physical Sciences, University of Sheffield, Hounsfield Road, Sheffield S37RH, U.K.*
[b] *Scuola Superiore Meridionale, Largo San Marcellino 10, 80138 Napoli, Italy*
[c] *INFN, Sezione di Napoli, Monte S. Angelo, Via Cintia, 80126 Napoli, Italy*
[d] *Department of Mathematics and Statistics, University of New Brunswick, Fredericton, NB, E3B 5A3, Canada*
[e] *Department of Physics, McGill University, Montréal, QC, H3A 2T8, Canada*

E-mail: y.zhai@sheffield.ac.uk, marco.decesare@na.infn.it, c.vandebruck@sheffield.ac.uk, e.divalentino@sheffield.ac.uk, edward.wilson-ewing@unb.ca

Abstract: We explore an interacting dark sector model in trace-free Einstein gravity where dark energy has a constant equation of state, $w = -1$, and the energy-momentum transfer potential is proportional to the cold dark matter density. Compared to the standard ΛCDM model, this scenario introduces a single additional dimensionless parameter, ϵ, which determines the amplitude of the transfer potential. Using a combination of *Planck* 2018 Cosmic Microwave Background (CMB), DESI 2024 Baryon Acoustic Oscillation (BAO), and Pantheon+ Type Ia supernovae (SNIa) data, we derive stringent constraints on the interaction, finding ϵ to be of the order of $\sim \mathcal{O}(10^{-4})$. While CMB and SNIa data alone do not favor the presence of such an interaction, the inclusion of DESI data introduces a mild 1σ preference for an energy-momentum transfer from dark matter to dark energy. This preference is primarily driven by DESI BAO measurements below redshift 1.4, which favor a slightly lower total matter density Ω_m compared to CMB constraints. Although the interaction remains weak and does not significantly alleviate the H_0 and S_8 tensions, our results highlight the potential role of dark sector interactions in late-time cosmology.

Keywords: CMBR theory, cosmological parameters from CMBR, dark energy theory, quantum gravity phenomenology

ArXiv ePrint: 2503.15659

https://doi.org/10.1088/1475-7516/2025/11/010

JCAP11(2025)010

Contents

1 Introduction

The Planck mission has marked the beginning of an exciting decade for cosmology, with its high-precision measurements of the cosmic microwave background [1–3]. The current understanding of the evolving Universe is built on a straightforward assumption of its homogeneity and isotropy, plus small inhomogeneous perturbations. Starting from this cornerstone, the widely accepted standard cosmological paradigm is the ΛCDM model based on general relativity, which assumes that dark matter is cold (CDM), single scalar-field inflation, and the existence of a cosmological constant (Λ) as the theoretical basis for the Universe's accelerated expansion. The ΛCDM model has been remarkably successful in explaining observations ranging from temperature and polarization anisotropies in the cosmic microwave background (CMB) [3–6], to the large-scale structure of the Universe [7, 8]; however, concerns about the ΛCDM model have been raised from both theoretical and observational perspectives since the model was first developed [9–12]. On one hand, the ΛCDM model suffers from the fine-tuning and coincidence problems [13]. The fine-tuning problem is that, assuming the ΛCDM model in data analysis, the derived cosmological constant is 54 orders of magnitude smaller than the vacuum energy predicted by quantum theory [14], while the coincidence problem is that today's energy density of total mass in the Universe, Ω_m, coincides in order of magnitude with that of the vacuum energy, Ω_Λ. On the other hand, the cosmological parameters measured from recent CMB observations disagree with those measured by local experiments at a 2–5σ level. Among these tensions, the discrepancies in the Hubble constant H_0 [15–25] and the matter clustering parameter $S_8 \equiv \sigma_8(\Omega_m/0.3)^{1/2}$ [26–43] stand out as the most significant.

Interacting dark energy (IDE) models have been proposed as a possible solution to these tensions [44–77]. Although certain phenomenological interactions between dark matter and dark energy have been found to relieve the tensions [68], they suffer from criticisms such as large-scale instability and dependence on non-local variables [78], like the Hubble parameter, which can be seen as a consequence of the first principle of thermodynamics [79].

Alternatively, the trace-free Einstein equations provide a minimal modification to the usual Einstein equations that naturally allows IDE models where dark energy has a constant

JCAP11(2025)010

equation of state $w = -1$ (similar to interacting vacuum models), and the energy-momentum transfer between dark matter and dark energy originates from a potential [80–82]. Importantly, these IDE models are not affected by the large-scale instability that plagues many IDE models [82, 83].

In general, the conservation of the matter stress-energy tensor does not follow from the trace-free Einstein equations but rather represents an independent assumption that leads to unimodular gravity, from which general relativity can be recovered with Λ playing the role of a free integration constant [84]. Instead, by allowing violations of the conservation of the matter stress-energy tensor, in the case where the energy-momentum loss is integrable, it is possible to recast the dynamics in the form of the usual Einstein field equations; however, now Λ is not a constant but rather a spacetime function [80, 81]. In this case, the trace-free Einstein equations must be complemented by a specific model for the energy-momentum transfer, which determines the evolution of Λ.

Within this context, it has been argued that energy-momentum non-conservation may arise due to diffusive interactions of low-energy matter degrees of freedom with the discrete quantum-gravity structures underlying spacetime [80]. Such non-conservation could potentially have an impact on cosmological scales, for example as a source of dark energy [85, 86], in alleviating the Hubble tension [81], the S_8 tension [87], and on the CMB [88].

In this paper, we derive constraints from cosmological datasets for a simple IDE model where the transfer potential is a linear function of the energy density of cold dark matter. Compared to ΛCDM, the model features an additional dimensionless free parameter ϵ, which represents the coupling strength between dark matter and dark energy and leads to an effective non-zero sound speed of dark matter (due to this effect, the model can equally be understood as a generalized dark matter model [89–92]). Requiring the absence of gradient instabilities ensures that energy flows from dark matter to dark energy, restricting ϵ to non-negative values.

The paper is organized as follows. In section 2, we review the formulation of the cosmological model at hand and its embedding within trace-free Einstein gravity. In section 3, we discuss the methodology used for the numerical simulations and data analysis. Our results are presented in section 4, where we discuss constraints on the parameters of the model. Finally, in section 5, we conclude and summarize our findings. A supplementary appendix A is also included, where we provide the dynamical equations for the cosmological background and perturbations in the synchronous gauge for a more general model with an arbitrary transfer potential.

2 Interactions in the dark sector

The trace-free Einstein equations

$$R_{ab} - \frac{1}{4} R\, g_{ab} = \kappa \left(T_{ab} - \frac{1}{4} T\, g_{ab}, \right) \tag{2.1}$$

where g_{ab} is the metric, R_{ab} is the Ricci curvature, $R = g^{ab} R_{ab}$ is the Ricci scalar, T_{ab} is the stress-energy tensor, $T = g^{ab} T_{ab}$ is the trace of the stress-energy tensor, and $\kappa \equiv 8\pi G$ is the gravitational coupling, are closely related to the standard Einstein equations, although with the important difference that, in this formulation, the stress-energy tensor is not necessarily conserved [84]. The energy-momentum transfer

$$J_a = \kappa \nabla^b T_{ab} \tag{2.2}$$

measures how strongly the conservation of the stress-energy tensor is violated. An interesting case occurs when the energy-momentum transfer is integrable, that is, $J_a = \nabla_a Q$ for some function Q, in which case it is possible to rewrite the trace-free Einstein equations as [80–82]

$$G_{ab} = \kappa T_{ab} + Q\, g_{ab}\,, \tag{2.3}$$

where $G_{ab} = R_{ab} - \frac{1}{2} R g_{ab}$ is the Einstein tensor, and $-Q$ can be seen as an *effective* cosmological constant, except that it is not constant, but rather a spacetime function. Note that, despite not being constant, Q nonetheless generates dark energy with an equation of state $w = -1$. Clearly, the Bianchi identities ensure that $\kappa \nabla^a T_{ab} + \nabla_a Q = 0$, so any variation in Q must be compensated for in T_{ab}. This provides a natural framework for an energy/momentum exchange between dark energy and dark matter. While models incorporating interactions with baryonic matter are possible, they would be tightly constrained by observations [93].

In this work, we constrain one such model where Q is linearly proportional to the energy density of CDM [82]:

$$Q = -\Lambda_{\rm f} + \kappa \epsilon \rho_c\,, \tag{2.4}$$

$$\delta Q = \kappa \epsilon\, \overline{\rho}_c \delta_c\,. \tag{2.5}$$

Here, $\Lambda_{\rm f}$ is an integration constant, ϵ is a dimensionless constant measuring the strength of the transfer from dark matter to dark energy, ρ_c is the energy density of cold dark matter which we split into background and perturbative pieces as $\rho_c = \overline{\rho}_c + \delta\rho_c$, and then $\delta_c = \delta\rho_c/\bar{\rho}_c$. This is one of the simplest models of energy transfer between the dark sectors, and it is, in fact, equivalent to generalized dark matter (GDM) models [89–92] with a constant equation of state [82]. We assume that only cold dark matter interacts with dark energy, so taking the divergence gives

$$\kappa \nabla^b T_{ab}^{\rm CDM} + \nabla_a Q = 0\,, \tag{2.6}$$

where $T_{ab}^{\rm CDM}$ is the stress-energy tensor for cold dark matter. Note that energy is transferred from dark matter to dark energy for the case $\epsilon > 0$, and in the reverse direction for $\epsilon < 0$. There is no transfer at all for $\epsilon = 0$, in which case $Q = \text{const}$.

This energy transfer modifies some of the equations of motion, both for the cosmological background and for the perturbations. Working in terms of the conformal time η, for which the Friedman-Lemaître-Robertson-Walker metric is $ds^2 = a(\eta)^2[-d\eta^2 + d\vec{x}^2]$ with $a(\eta)$ being the scale factor, the equations for the background become

$$\mathcal{H}^2 = \frac{a^2}{3}\left(\kappa\overline{\rho} - \epsilon\kappa\overline{\rho}_c + \Lambda_{\rm f}\right)\,, \tag{2.7}$$

$$\mathcal{H}^2 + 2\mathcal{H}' = -a^2\left(\kappa\overline{p} + \epsilon\kappa\overline{\rho}_c - \Lambda_{\rm f}\right)\,, \tag{2.8}$$

$$(1-\epsilon)\overline{\rho}_c' + 3\mathcal{H}\overline{\rho}_c = 0\,, \tag{2.9}$$

where $\mathcal{H} = a'/a$, and primes denote derivatives with respect to η. For the perturbations, in terms of Fourier modes in the synchronous gauge,

$$\delta_c' = -\frac{1}{1-\epsilon}\left(\theta_c + \frac{h'}{2}\right), \tag{2.10}$$

$$\theta_c' = -\frac{1-4\epsilon}{1-\epsilon}\mathcal{H}\theta_c + \epsilon k^2 \delta_c\,, \tag{2.11}$$

where k is the norm of the Fourier mode, θ_c is the velocity perturbation of cold dark matter, and h is the trace of the metric perturbation in the synchronous gauge (and recall that $\delta_c = \delta\rho_c/\overline{\rho}_c$); for the precise definition of these quantities see, e.g., [94].

In addition to dark matter (treated as pressureless dust), T_{ab} receives contributions from baryons and radiation (photons and neutrinos), while, as explained above, Q is the source of dark energy. The remaining equations of motion are given in appendix A. The dynamics of tensor perturbations are unaffected, and the only deviations from ΛCDM appear in the scalar sector.

Many interacting dark energy models with $w \neq -1$ are affected by a large-scale instability, which gives rise to a runaway growth of the velocity perturbation of dark energy, $\theta_{\rm DE}$ [83]. However, since in this framework dark energy has $w = -1$, it is not necessary to define its four-velocity or its perturbation $\theta_{\rm DE}$, since the four-velocity does not appear in the equations of motion (the contribution to the right-hand side of (2.3) from dark energy is independent of its four-velocity). In such a case, the instability results obtained in ref. [83] no longer necessarily apply, and, in particular, the model considered here is free of this instability [82], and we expect this will continue to be true for a large class of functions Q.

Note that the family of IDE models we consider here assumes a particular scalar function Q, which is identified with $-\Lambda_{\rm eff}$ [82]. This convention differs from the standard literature, where $\tilde{Q}$ (adding a tilde to avoid confusion) instead denotes the interaction between CDM and dark energy; the relation is $\tilde{Q} = \overline{Q}'/\kappa$. For common choices in the literature, such as $\tilde{Q} = H$, Q would be an integral of H over time and be non-local in time.

Furthermore, in the cases studied so far, the requirement that there should be no gradient instabilities on sub-horizon scales often determines the sign of the coupling. For this model, this requirement gives $\epsilon > 0$, since the effective sound speed of the interacting dark matter is $c^2_{s,\rm eff} = \epsilon/(1-\epsilon)$ [82]. In turn, this implies that $\overline{Q}' < 0$: energy must flow from dark matter to dark energy.

Lastly, we note that the trace-free Einstein equations (2.1) may also be derived from an action principle by imposing the additional requirement of invariance under volume-preserving diffeomorphisms [95]. This is known as unimodular gravity, but it comes with an additional condition, the so-called unimodularity constraint, that fixes the volume element to a non-dynamical background quantity. In this study, following [82], we work with the field equations (2.1) without imposing the unimodularity condition, thus retaining full gauge invariance. For technical aspects concerning the relation between unimodular gravity and trace-free Einstein gravity, specifically concerning gauge invariance, see refs. [96, 97] and references therein. Alternative action functionals that give the trace-free field equations (2.1) have been formulated in refs. [98, 99]; however, due to the diffusive nature of interactions in the general framework considered here, an action principle formulation for IDE models based on the trace-free Einstein equations may not be available.

3 Methodology and data

We analyzed the posterior distributions obtained using the publicly available Bayesian analysis code `COBAYA`, which was developed based on its predecessor `CosmoMC`, while a fast-dragging algorithm was implemented for efficient oversampling of the fast parameters — usually experimental nuisance parameters [100, 101]. `COBAYA` allows us to combine the modified cosmological theory and experimental likelihoods with the Markov Chain Monte Carlo (MCMC) sampling algorithm. To calculate the predictions of the model under consideration, we exploit a modified version of the Cosmic Linear Anisotropy Solving System code (`CLASS`) [102]. In our modified code, we updated the dark matter perturbation equations (according to (2.10) and (2.11)) and the gravitational field equations (according to (A.8) and (A.9)) to be in concordance with the IDE model in this work. The dynamical equations for the cosmological background and perturbations in the synchronous gauge are reviewed in appendix A. The parameters being sampled are the ϵ parameter, denoting the interaction, and the six parameters from the baseline ΛCDM model, namely, the baryon energy density $\Omega_b h^2$, the cold dark matter energy density $\Omega_c h^2$, the angular size of the sound horizon at recombination θ_s, the optical depth at reionization τ, the primordial scalar power spectrum amplitude A_s, and the spectral index n_s. Since the $\epsilon < 0$ regime is not of interest in this work due to its gradient instability, we assume a flat prior on $\epsilon \in [0, 0.1]$. In table 1, we list the priors applied to the parameters in our model.

The datasets used in this work are as follows:

- The full *Planck* 2018 temperature and polarization likelihoods [3, 103, 104], together with the *Planck* 2018 lensing likelihood [105]. We refer to this dataset as **Planck2018**.

- The full *Planck* 2018 temperature and polarization likelihoods [3, 103, 104], together with the *Planck* 2018 lensing likelihood [105], combined with DESI Baryon Acoustic Oscillation (BAO) distance measurements from galaxies and quasars [106–108]. For each sample at its effective redshift z, either both the transverse comoving distance D_M/r_d and Hubble horizon D_H/r_d or the angle-averaged distance D_V/r_d is measured by DESI, where distance measurements are scaled by r_d. The full list of samples is given in ref. [108]. We refer to this dataset as **Planck2018+DESI**.

- The full *Planck* 2018 temperature and polarization likelihoods [3, 103, 104], together with the *Planck* 2018 lensing likelihood [105], combined with the Pantheon+ likelihood [109]. The Pantheon+ likelihood is obtained by analyzing 1701 light curves from 1550 Type Ia supernovae. We refer to this dataset as **Planck2018+SNIa**.

- The full *Planck* 2018 temperature and polarization likelihoods [3, 103, 104], together with the *Planck* 2018 lensing likelihood [105], combined with DESI Baryon Acoustic Oscillation (BAO) data [106–108] and the Pantheon+ likelihood [109]. We refer to this dataset as **Planck2018+DESI+SNIa**.

JCAP11(2025)010

Parameter	Prior
$\Omega_{\rm b}h^2$	$[0.005, 0.1]$
$\Omega_{\rm c}h^2$	$[0.001, 0.990]$
$\tau_{\rm reio}$	$[0.01, 0.80]$
$n_{\rm s}$	$[0.8, 1.2]$
$\log(10^{10}A_{\rm s})$	$[1.61, 3.91]$
$100\theta_{\rm s}$	$[0.5, 10]$
ϵ	$[0, 0.1]$

Table 1. Flat priors on the parameters sampled in the MCMC analysis.

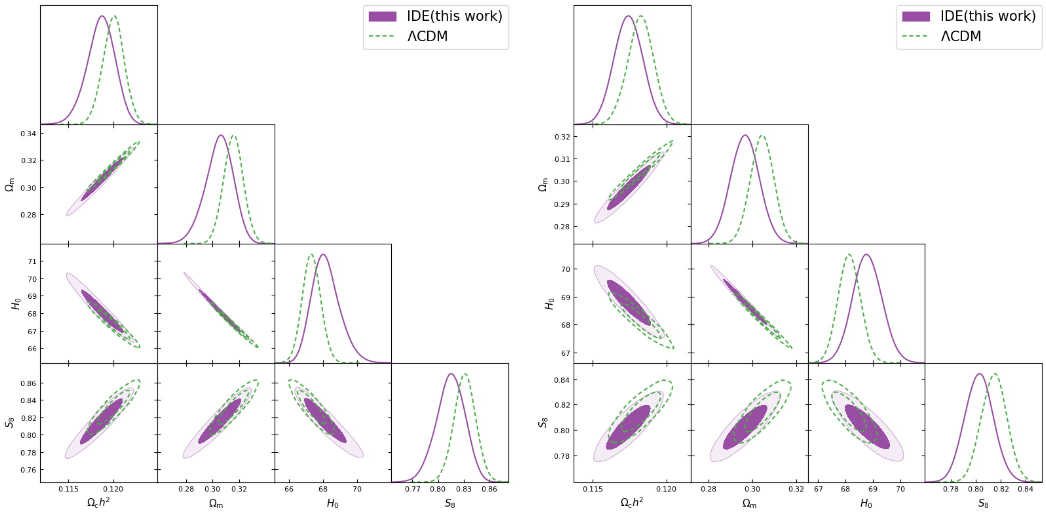

Figure 1. The left (right) posterior distributions show constraints on fiducial ΛCDM model and the model in this work from Planck2018 (Planck2018+DESI).

A modified version of the Gelman-Rubin statistic, $R - 1$, is adopted in `COBAYA` to measure chain sampling convergence [100, 110]. We set the criterion for chain convergence at $R - 1 < 0.02$.

4 Results

The constraints at the 68% (95%) confidence level (CL) on the parameters of the present model are presented in table 2. Comparing our results with those obtained by assuming a ΛCDM model, we observe a shift of about 1σ in the cold dark matter density, and consequently in the total matter density, towards smaller values, as shown in figure 1. This occurs because ϵ is negatively correlated with these parameters, as we can see in figure 2. As a result, due to the very accurate measurements of $\Omega_m h^2$ from the CMB peaks, ϵ is positively correlated with H_0, which also shifts towards higher values by approximately 1σ. The key feature of the results is that the scale of the dimensionless interaction parameter ϵ is small, on the order of $\sim \mathcal{O}(10^{-4})$, and consistent with no interaction for Planck2018 only, with $\epsilon < 9 \times 10^{-4}$ at 95% CL. This is expected because the interaction in this model is proportional to the energy

JCAP11(2025)010

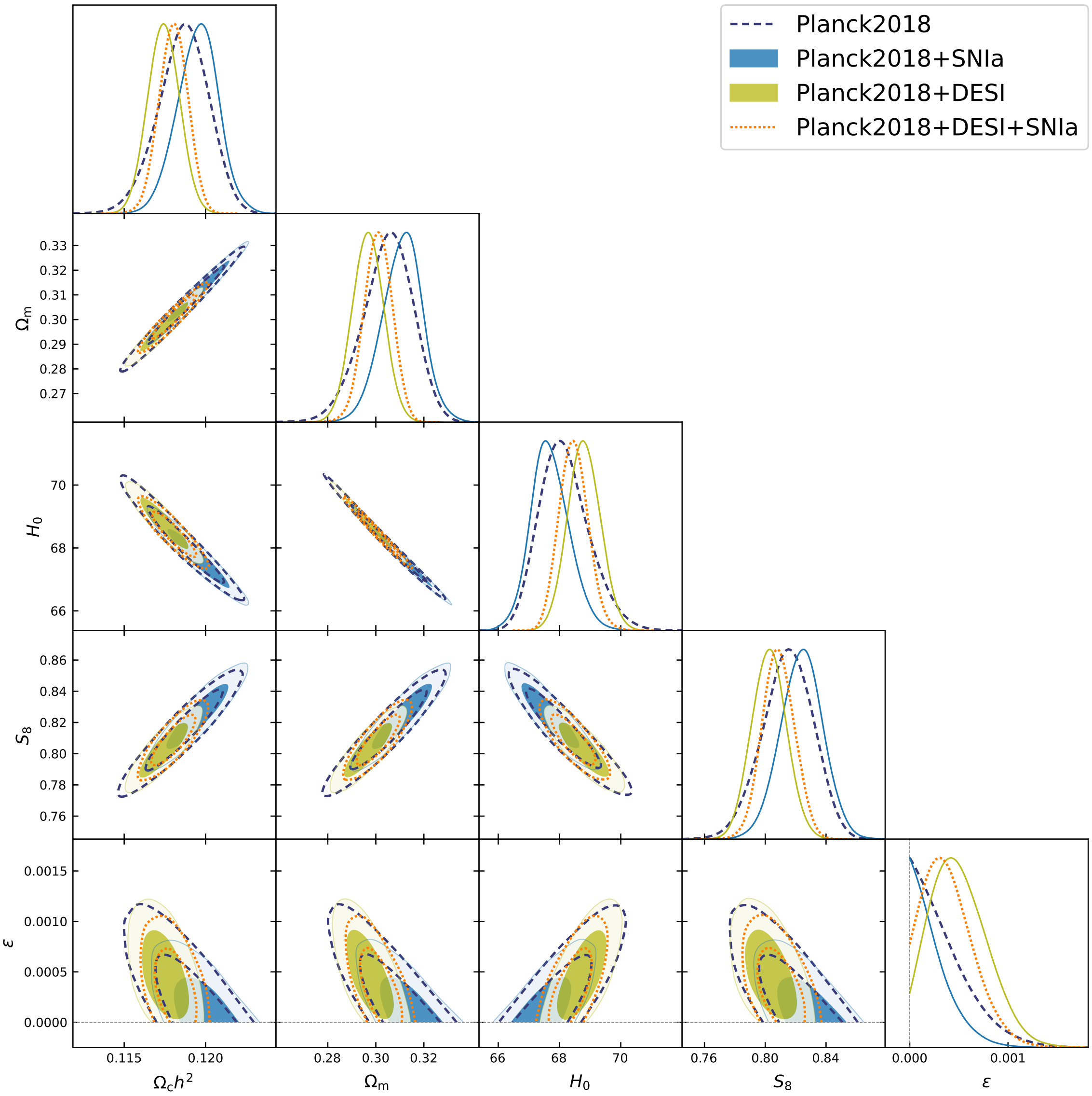

Figure 2. The posterior distributions of the interacting dark energy model across different dataset combinations. We apply a prior $\epsilon \in [0, 0.1]$, motivated by theoretical instabilities that arise for negative ϵ values. The results are not affected by imposing such positive prior on ϵ, as discussed further in this section.

density of dark matter, ρ_c, as shown in eq. (2.5). In the literature, interacting dark energy models with similar ρ_c-dependence exhibit comparably tight constraints on their interaction parameters. Their posterior distributions are concentrated close to zero, as analyzed using various combinations of datasets [44]. The main reason for such small derived values is that, as shown in figure 3, introducing a stronger interaction in the cosmological model reduces the amplitudes of the peaks. These peaks are very well constrained by data, as this region has very small error bars. Meanwhile, the predicted Sachs-Wolfe plateau at low multipoles increases; however, this lies in the cosmic variance-limited region, where the error bars are large and the effect is less significant. The decrease in peak amplitudes is

JCAP11(2025)010

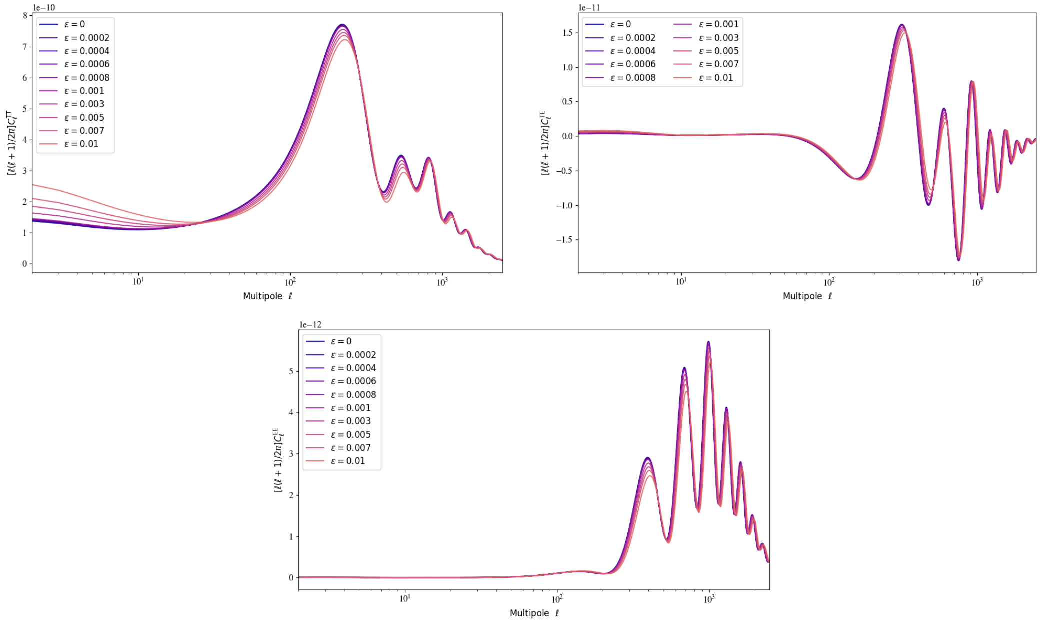

Figure 3. The theoretical predictions on the CMB TT, TE, EE power spectra for various ϵ values.

consistent across the CMB TT, TE, and EE spectra. The *Planck* mission measures these peaks with high precision, leaving very little tolerance for such mechanisms. This effect is very similar to the constraints on the Hubble constant, where a larger H_0 value also leads to smaller peaks. In figure 2, the correlation between ϵ and H_0 can be examined more straightforwardly. These findings also remain robust when tested with *Planck* PR4 data [111–113], which yield consistent results.

A different effect is observed in the DESI-combined analyses, which prefer a higher ϵ value. This is due to the preference of DESI 2024 BAO measurements for lower values of Ω_m, which breaks degeneracies in the parameter space, slightly favoring higher values of the interaction parameter: $\epsilon = 0.00049^{+0.00022}_{-0.00033}$ at 68% CL for Planck2018+DESI and $\epsilon = 0.00041^{+0.00015}_{-0.00035}$ at 68% CL for Planck2018+DESI+SNIa. Compared to CMB results, DESI data alone favor a smaller total matter density when assuming a constant dark energy equation of state. In the ΛCDM scenario, the derived total matter densities from Planck2018+DESI and DESI alone are $\Omega_m = 0.3069 \pm 0.0050$ and 0.295 ± 0.015, respectively. This preference for a smaller Ω_m in DESI is mainly driven by the DESI distance measurements at lower redshift bins ($z \leq 1.4$), more explicitly by the bright galaxy sample (BGS), luminous red galaxies (LRG), and emission line galaxies (ELG), as shown in figure 4 [108]. It is interesting to note that the LRG and ELG tracers at the same redshift bins are cross-correlated in their clustering analyses, in which BAO measurements from other redshift bins are not involved. This trend in the redshift range $z \leq 1.4$ is not masked by data from higher-redshift bins. Moreover, the DESI-combined datasets show a strong preference for a time-varying dark energy equation of state at levels $\geq 2.5\sigma$ [108, 114], while in this work based on the trace-free Einstein equations $w = -1$. Overall, the DESI 2024 BAO data break degeneracies present in CMB analyses, such as the Ω_m-H_0-w degeneracy, leading to a decreasing trend in Ω_m. When an interaction

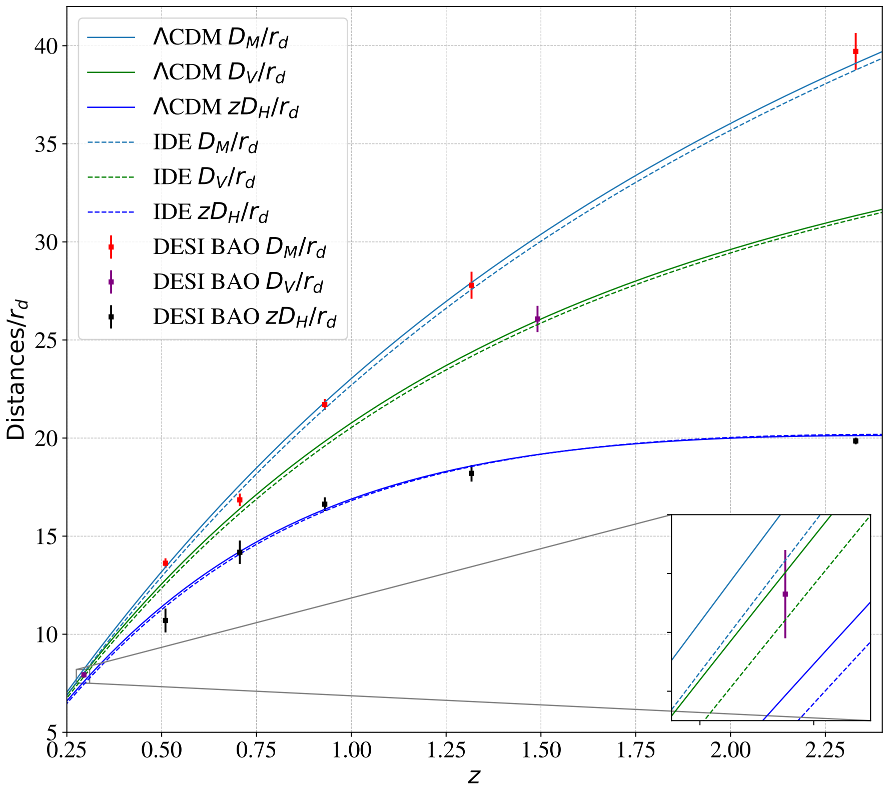

Figure 4. Distance-redshift relations from the Planck2018+DESI dataset, adopting the IDE (ΛCDM) best-fit, are shown with dashed (solid) lines. The y-axis is rescaled by the sound horizon at baryon drag, r_d. For visual convenience, D_H/r_d is further rescaled by z. The sample points represent DESI 2024 BAO distance measurements, with corresponding $\pm 1\sigma$ uncertainties. From low to high redshifts, these plotted samples include BGS at $0.1 < z < 0.4$, LRG at $0.4 < z < 0.6$, LRG at $0.6 < z < 0.8$, a combined sample of LRG and ELG at the overlapping redshift range $0.8 < z < 1.1$, ELG at $1.1 < z < 1.6$, quasars at $0.8 < z < 2.1$, and quasars at $1.77 < z < 4.16$.

between dark sectors is allowed, this degeneracy-breaking effect induces significant changes in the posterior distribution, resulting in a nonzero ϵ.

For exactly the opposite reason, i.e., because they prefer a higher value for the matter density, SNIa data are more in agreement with no interaction at all. The upper limit on $\epsilon < 6 \times 10^{-4}$ at 95% CL for Planck2018+SNIa is stronger than in the Planck2018 case alone, and for the same reason, the Hubble constant shifts towards a lower value, making it more consistent with the ΛCDM case. However, as explained above, the compromise found with DESI BAO data indicates an interaction different from zero at 1σ, even when SNIa data are included in the full dataset combination.

Due to correlations between ϵ, H_0, Ω_m, and the assumptions on the dark energy equation of state, it is also interesting to compare with interacting dark energy models in the literature with energy transfer from DM to DE and their effects on the tensions [51, 115–117]. In the ΛCDM scenario, CMB data suggest a relatively large Ω_m. When CMB data are involved, the energy-momentum transfer from dark matter to dark energy due to their interaction can naturally reduce Ω_m, leading to a larger current expansion rate and, consequently, mitigating

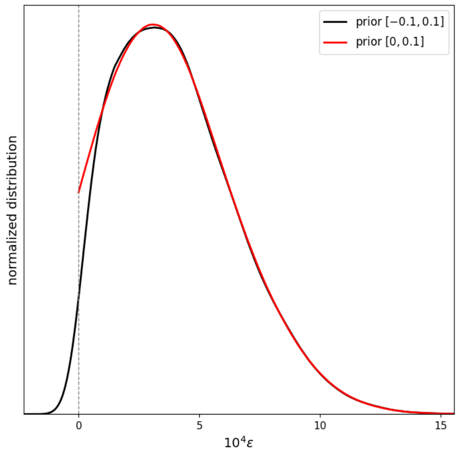

Figure 5. By adopting flat priors of [-0.1, 0.1] and [0, 0.1], the normalized ϵ posterior distributions are plotted in black and red, respectively. The likelihoods are the Planck2018+DESI+SNIa dataset.

the H_0 tension. For the same reason, if late-time measurements such as DESI 2024 BAO are combined — where a smaller Ω_m is observed — such an interaction is more supported by data analysis. Conversely, when SNIa data are included, which prefer a higher Ω_m, the interaction is in disagreement with the data. By relaxing the assumptions on the dark energy equation of state, either by assuming a constant $w \neq -1$ or allowing w to vary with time, the low-redshift tension on Ω_m is alleviated [118]. In this case, the constraints on the interaction are loosened, and the intensity of such an interaction becomes less significant [52, 64, 119]. It remains challenging to reconcile all measurements simultaneously, as the constraints on dark-sector interactions from matter clustering and the expansion rate measured by early- and late-time projects are engaged in an arm-wrestling match.

The simple model analyzed here does not address the H_0 and S_8 tensions. We note that, despite some similarities between the model at hand and the 'anomalous diffusion' model considered in ref. [81], which was proposed to alleviate the Hubble tension, the latter features a step function in the transfer potential, such that the (effective) equation of state of cold dark matter undergoes a sharp transition at recombination, an effect that is absent in the present model (2.4). Extensions of the present model, including such sudden transitions, will be investigated in future work.

Lastly, we remark that in this work, we assumed a non-negative flat prior for ϵ due to the gradient instability in the $\epsilon < 0$ case [82]. On the other hand, if we allow for negative ϵ values and assume a flat prior in the interval $[-0.1, 0.1]$, the posterior distribution features a sharp tail at the lower boundary; see figure 5. This is consistent with the findings in ref. [82], which indicate that the $\epsilon < 0$ case is problematic, and it further shows that this regime is also disfavored by data.

5 Conclusions

We have conducted a comprehensive analysis of a dark sector interaction model based on the trace-free Einstein equations where the energy-momentum transfer potential is proportional to

Parameter	Planck2018	Planck2018+DESI	Planck2018+SNIa	Planck2018+DESI+SNIa
$\Omega_{\rm b}h^2$	0.02232 ± 0.00015	0.02236 ± 0.00016	0.02230 ± 0.00015	0.02234 ± 0.00015
$\Omega_{\rm c}h^2$	$0.1186^{+0.0017}_{-0.0014}$	0.11742 ± 0.00097	$0.1195^{+0.0013}_{-0.0012}$	0.11802 ± 0.00088
$\tau_{\rm reio}$	0.0543 ± 0.0077	0.0564 ± 0.0073	0.0530 ± 0.0072	0.0553 ± 0.0071
$n_{\rm s}$	0.9660 ± 0.0043	0.9683 ± 0.0036	0.9645 ± 0.0040	0.9673 ± 0.0035
$\log(10^{10}A_{\rm s})$	3.043 ± 0.015	3.046 ± 0.014	3.042 ± 0.014	3.044 ± 0.014
H_0	$68.17^{+0.67}_{-0.92}$	68.80 ± 0.53	$67.73^{+0.56}_{-0.67}$	68.46 ± 0.47
$\Omega_{\rm m}$	$0.305^{+0.011}_{-0.009}$	0.2967 ± 0.0065	$0.3107^{+0.0088}_{-0.0076}$	0.3009 ± 0.0058
σ_8	0.8083 ± 0.0060	0.8070 ± 0.0060	0.8095 ± 0.0058	0.8074 ± 0.0058
S_8	$0.815^{+0.018}_{-0.015}$	0.803 ± 0.011	0.824 ± 0.014	0.809 ± 0.011
ϵ	$< 0.000436 (< 0.000926)$	$0.00049^{+0.00022}_{-0.00033} (< 0.00097)$	$< 0.000292 (< 0.000637)$	$0.00040^{+0.00015}_{-0.00034} (< 0.000868)$
$\Delta\chi^2_{\rm min}$	1.67	−2.27	−1.33	−1.31
ΔAIC	3.67	−0.27	0.67	0.69

Table 2. Constraints at 68% (95%) CL on parameters from various combinations of datasets. Here $\Delta\chi^2_{\rm min} = \chi^2_{\rm min,\ IDE} - \chi^2_{\rm min,\ \Lambda CDM}$, so that a negative $\Delta\chi^2_{\rm min}$ indicates the IDE model provides a better fit than ΛCDM to the dataset. The Akaike Information Criterion, $\mathrm{AIC} = 2k + \chi^2$ is provided, where k is the number of parameters in the model. $\Delta\mathrm{AIC} = \mathrm{AIC}_{\rm IDE} - \mathrm{AIC}_{\Lambda CDM}$.

the cold dark matter density. Using a combination of *Planck* 2018 CMB, DESI 2024 BAO, and Pantheon+ SNIa data, we derived tight constraints on the interaction strength, characterized by the dimensionless parameter ϵ. Our results show that ϵ is of the order of $\sim \mathcal{O}(10^{-4})$, with no significant evidence of interaction from CMB and SNIa data alone. However, when DESI data are included, a mild 1σ preference emerges for an energy-momentum transfer from dark matter to dark energy, with $\epsilon \approx (4\text{–}5) \times 10^{-4}$. This preference is primarily driven by the lower Ω_m values favored by low-redshift DESI BAO measurements.

Despite this indication, the interaction remains small and does not significantly alleviate the Hubble constant (H_0) or matter clustering (S_8) tensions. Nevertheless, our findings reinforce the idea that late-time interactions in the dark sector could have subtle yet measurable effects on the expansion history and structure formation. The observed correlation between ϵ and Ω_m suggests that further investigations into IDE models may yield new insights into potential modifications to the standard ΛCDM paradigm.

Trace-free Einstein gravity provides a minimal modification to general relativity that is covariant, and naturally allows a large class of IDE models. While our analysis here focused on a simple interaction model with a linear dependence on the cold dark matter energy density, a broader class of IDE models remains largely unexplored. One potential avenue for future research is the inclusion of more general transfer functions Q, allowing for time-dependent or scale-dependent interactions. Such extensions could potentially provide a better fit to data while simultaneously preserving key features of the standard cosmological model.

Additionally, the preference for interaction in the DESI BAO data — though not statistically strong — suggests that future large-scale structure surveys may be crucial in testing IDE scenarios. The upcoming Euclid mission, the Vera C. Rubin Observatory's LSST

JCAP11(2025)010

survey, and future DESI data releases will significantly refine BAO and large-scale structure constraints, allowing for more precise measurements of Ω_m, H_0, and dark sector interactions. Continued theoretical advancements and observational progress will be key to determining whether such interactions play a fundamental role in shaping the evolution of the universe.

Acknowledgments

MdC acknowledges support from INFN iniziativa specifica GeoSymQFT. CvdB is supported by the Lancaster-Sheffield Consortium for Fundamental Physics under STFC grant: ST/X000621/1. EDV acknowledges support from the Royal Society through a Royal Society Dorothy Hodgkin Research Fellowship. The work of EWE is supported in part by the Natural Sciences and Engineering Research Council of Canada. This work contributes to COST Action CA21136 — Addressing observational tensions in cosmology with systematics and fundamental physics (CosmoVerse). We acknowledge IT Services at The University of Sheffield for the provision of services for High Performance Computing.

JCAP11(2025)010

A System of equations of motion

In this appendix, we review the cosmological dynamics for the class of models at hand with a general transfer potential Q. We specialize the results of ref. [82] to the synchronous gauge and re-express the equations using the notation of ref. [94], which is convenient for implementation in the `CLASS` code. The dynamical equations for the particular model considered in this paper can be obtained by substituting eq. (2.4) into the equations shown below.

The Friedmann equations and the continuity equations, with a general transfer potential, can be split, as usual, into background and perturbative degrees of freedom. Assuming a spatially flat FLRW background, the equations of motion for the background degrees of freedom are, in conformal time,

$$\mathcal{H}^2 = \frac{a^2}{3}\left(\kappa\overline{\rho} - \overline{Q}\right) , \quad \mathcal{H}^2 + 2\mathcal{H}' = -a^2\left(\kappa\overline{p} + \overline{Q}\right) , \tag{A.1}$$

$$\overline{\rho}'_\gamma + 4\mathcal{H}\overline{\rho}_\gamma = 0 , \qquad \overline{\rho}'_\nu + 4\mathcal{H}\overline{\rho}_\nu = 0 , \tag{A.2}$$

$$\overline{\rho}'_b + 3\mathcal{H}\overline{\rho}_b = 0 , \qquad \overline{\rho}'_c + 3\mathcal{H}\overline{\rho}_c = \frac{\overline{Q}'}{\kappa} , \tag{A.3}$$

where $\mathcal{H}$ is the conformal Hubble rate and primes denote derivatives with respect to conformal time. The indices are: γ for radiation, ν for neutrinos, b for baryonic matter, and c for cold dark matter, while the total energy density is

$$\overline{\rho} = \overline{\rho}_\gamma + \overline{\rho}_\nu + \overline{\rho}_b + \overline{\rho}_c , \tag{A.4}$$

and the total pressure is

$$\overline{p} = \frac{1}{3}\left(\overline{\rho}_\gamma + \overline{\rho}_\nu\right) . \tag{A.5}$$

For scalar perturbations, we work in the synchronous gauge and use the same conventions as in ref. [83], where the line element is

$$\mathrm{d}s^2 = a^2\Big(- \mathrm{d}\tau^2 + [(1-2\psi)\delta_{ij} + 2E_{,ij}]\mathrm{d}x^i\mathrm{d}x^j\Big) . \tag{A.6}$$

The general case has been worked out in ref. [82], from which the equations shown below can be obtained by imposing the gauge conditions $B = \phi = 0$. In Fourier space, we have the following correspondence with the variables h, η used in ref. [94]:

$$\psi = \eta\,, \quad E = -\frac{1}{2k^2}\,(h + 6\eta)\;. \tag{A.7}$$

In terms of these variables, the gravitational field equations read

$$2k^2\eta - \mathcal{H}h' = -a^2\,(\kappa\delta\rho - \delta Q)\;, \tag{A.8}$$

$$k^2\eta' = \frac{\kappa}{2}a^2(\overline{\rho} + \overline{p})\theta\;, \tag{A.9}$$

$$h'' + 2\mathcal{H}h' - 2k^2\eta = -3a^2\,(\kappa\delta p + \delta Q)\;, \tag{A.10}$$

$$h'' + 6\eta'' + 2\mathcal{H}(h' + 6\eta') - 2k^2\eta = -2\kappa a^2 k^2\pi\,. \tag{A.11}$$

We assume that the matter fields considered here have no intrinsic entropy perturbations, that is, $c_{s\,A}^2 = c_{a\,A}^2 = w_A$. Then, the perturbed continuity equations (including Thomson scattering and neglecting the contribution of photons to the anisotropic stress) are

$$\delta'_\gamma + \frac{4}{3}\theta_\gamma + \frac{2}{3}h' = 0\,, \qquad \delta'_\nu + \frac{4}{3}\theta_\nu + \frac{2}{3}h' = 0\,, \tag{A.12}$$

$$\delta'_b + \theta_b + \frac{h'}{2} = 0\,, \qquad \delta'_c + \theta_c + \frac{h'}{2} = \frac{\delta Q' - \bar{Q}'\delta_c}{\kappa\bar{\rho}_c}\,, \tag{A.13}$$

$$\theta'_\gamma - \frac{k^2}{4}\delta_\gamma = \tau_c^{-1}(\theta_b - \theta_\gamma)\,, \qquad \theta'_\nu - \frac{k^2}{4}\delta_\nu + k^2\sigma_\nu = 0\,, \tag{A.14}$$

$$\theta'_b + \mathcal{H}\theta_b - k^2 c_{s,b}^2\delta_b = \left(\frac{4\bar{\rho}_\gamma}{3\bar{\rho}_b}\right)\,\tau_c^{-1}(\theta_\gamma - \theta_b)\,, \qquad \theta'_c + \mathcal{H}\theta_c = \frac{k^2\delta Q - \bar{Q}'\theta_c}{\kappa\bar{\rho}_c}\,, \tag{A.15}$$

where $\tau_c = (an_e\sigma_T)^{-1}$ and $\sigma_\nu = \left(2k^2/3(\bar{\rho}_\nu + \bar{p}_\nu)\right)\pi_\nu = \left(k^2/2\bar{\rho}_\nu\right)\pi_\nu$. The equation for σ_ν is obtained from the quadrupolar moment of the Boltzmann equation [94] (we neglect the neutrino octopole term, following ref. [83])

$$\sigma'_\nu = \frac{4}{15}\theta_\nu\,. \tag{A.16}$$

References

[1] Planck collaboration, *Planck 2013 results. I. Overview of products and scientific results*, *Astron. Astrophys.* **571** (2014) A1 [arXiv:1303.5062] [inSPIRE].

[2] Planck collaboration, *Planck 2013 results. XVI. Cosmological parameters*, *Astron. Astrophys.* **571** (2014) A16 [arXiv:1303.5076] [inSPIRE].

[3] Planck collaboration, *Planck 2018 results. VI. Cosmological parameters*, *Astron. Astrophys.* **641** (2020) A6 [*Erratum ibid.* **652** (2021) C4] [arXiv:1807.06209] [inSPIRE].

[4] ACT collaboration, *The Atacama Cosmology Telescope: DR4 Maps and Cosmological Parameters*, *JCAP* **12** (2020) 047 [arXiv:2007.07288] [inSPIRE].

[5] SPT-3G collaboration, *Measurements of the E-mode polarization and temperature-E-mode correlation of the CMB from SPT-3G 2018 data*, *Phys. Rev. D* **104** (2021) 022003 [arXiv:2101.01684] [inSPIRE].

[6] SPT-3G collaboration, *Measurement of the CMB temperature power spectrum and constraints on cosmology from the SPT-3G 2018 TT, TE, and EE dataset*, Phys. Rev. D **108** (2023) 023510 [arXiv:2212.05642] [INSPIRE].

[7] DES collaboration, *Dark Energy Survey Year 1 results: Cosmological constraints from cosmic shear*, Phys. Rev. D **98** (2018) 043528 [arXiv:1708.01538] [INSPIRE].

[8] eBOSS collaboration, *Completed SDSS-IV extended Baryon Oscillation Spectroscopic Survey: Cosmological implications from two decades of spectroscopic surveys at the Apache Point Observatory*, Phys. Rev. D **103** (2021) 083533 [arXiv:2007.08991] [INSPIRE].

[9] L. Perivolaropoulos and F. Skara, *Challenges for ΛCDM: An update*, New Astron. Rev. **95** (2022) 101659 [arXiv:2105.05208] [INSPIRE].

[10] E. Abdalla et al., *Cosmology intertwined: A review of the particle physics, astrophysics, and cosmology associated with the cosmological tensions and anomalies*, JHEAp **34** (2022) 49 [arXiv:2203.06142] [INSPIRE].

[11] E. Di Valentino, *Challenges of the Standard Cosmological Model*, Universe **8** (2022) 399 [INSPIRE].

[12] P.J.E. Peebles, *Status of the LambdaCDM theory: supporting evidence and anomalies*, arXiv:2405.18307 [INSPIRE].

[13] S. Weinberg, *The Cosmological Constant Problem*, Rev. Mod. Phys. **61** (1989) 1 [INSPIRE].

[14] J. Martin, *Everything You Always Wanted To Know About The Cosmological Constant Problem (But Were Afraid To Ask)*, Comptes Rendus Physique **13** (2012) 566 [arXiv:1205.3365] [INSPIRE].

[15] L. Verde, T. Treu and A.G. Riess, *Tensions between the Early and the Late Universe*, Nature Astron. **3** (2019) 891 [arXiv:1907.10625] [INSPIRE].

[16] E. Di Valentino et al., *Snowmass2021 — Letter of interest cosmology intertwined II: The hubble constant tension*, Astropart. Phys. **131** (2021) 102605 [arXiv:2008.11284] [INSPIRE].

[17] E. Di Valentino et al., *In the realm of the Hubble tension — a review of solutions*, Class. Quant. Grav. **38** (2021) 153001 [arXiv:2103.01183] [INSPIRE].

[18] N. Schöneberg et al., *The H0 Olympics: A fair ranking of proposed models*, Phys. Rept. **984** (2022) 1 [arXiv:2107.10291] [INSPIRE].

[19] P. Shah, P. Lemos and O. Lahav, *A buyer's guide to the Hubble constant*, Astron. Astrophys. Rev. **29** (2021) 9 [arXiv:2109.01161] [INSPIRE].

[20] M. Kamionkowski and A.G. Riess, *The Hubble Tension and Early Dark Energy*, Ann. Rev. Nucl. Part. Sci. **73** (2023) 153 [arXiv:2211.04492] [INSPIRE].

[21] W. Giarè, *CMB Anomalies and the Hubble Tension*, arXiv:2305.16919 [DOI:10.1007/978-981-99-0177-7_36] [INSPIRE].

[22] J.-P. Hu and F.-Y. Wang, *Hubble Tension: The Evidence of New Physics*, Universe **9** (2023) 94 [arXiv:2302.05709] [INSPIRE].

[23] L. Verde, N. Schöneberg and H. Gil-Marín, *A tale of many H_0*, arXiv:2311.13305.

[24] E. Di Valentino and D. Brout, *The Hubble Constant Tension*, Springer (2024) [DOI:10.1007/978-981-99-0177-7] [INSPIRE].

[25] L. Perivolaropoulos, *Hubble tension or distance ladder crisis?*, Phys. Rev. D **110** (2024) 123518 [arXiv:2408.11031] [INSPIRE].

[26] E. Di Valentino et al., *Cosmology Intertwined III: $f\sigma_8$ and S_8*, *Astropart. Phys.* **131** (2021) 102604 [arXiv:2008.11285] [INSPIRE].

[27] E. Di Valentino and S. Bridle, *Exploring the Tension between Current Cosmic Microwave Background and Cosmic Shear Data*, *Symmetry* **10** (2018) 585 [INSPIRE].

[28] DES collaboration, *Dark Energy Survey Year 3 results: Cosmology from cosmic shear and robustness to data calibration*, *Phys. Rev. D* **105** (2022) 023514 [arXiv:2105.13543] [INSPIRE].

[29] DES collaboration, *Dark Energy Survey Year 3 results: Cosmology from cosmic shear and robustness to modeling uncertainty*, *Phys. Rev. D* **105** (2022) 023515 [arXiv:2105.13544] [INSPIRE].

[30] KiDS collaboration, *KiDS-1000 Cosmology: Cosmic shear constraints and comparison between two point statistics*, *Astron. Astrophys.* **645** (2021) A104 [arXiv:2007.15633] [INSPIRE].

[31] M. Asgari et al., *KiDS+VIKING-450 and DES-Y1 combined: Mitigating baryon feedback uncertainty with COSEBIs*, *Astron. Astrophys.* **634** (2020) A127 [arXiv:1910.05336] [INSPIRE].

[32] S. Joudaki et al., *KiDS+VIKING-450 and DES-Y1 combined: Cosmology with cosmic shear*, *Astron. Astrophys.* **638** (2020) L1 [arXiv:1906.09262] [INSPIRE].

[33] G. D'Amico et al., *The Cosmological Analysis of the SDSS/BOSS data from the Effective Field Theory of Large-Scale Structure*, *JCAP* **05** (2020) 005 [arXiv:1909.05271] [INSPIRE].

[34] Kilo-Degree Survey and DES collaborations, *DES Y3 + KiDS-1000: Consistent cosmology combining cosmic shear surveys*, *Open J. Astrophys.* **6** (2023) 2305.17173 [arXiv:2305.17173] [INSPIRE].

[35] T. Tröster et al., *Cosmology from large-scale structure: Constraining ΛCDM with BOSS*, *Astron. Astrophys.* **633** (2020) L10 [arXiv:1909.11006] [INSPIRE].

[36] C. Heymans et al., *KiDS-1000 Cosmology: Multi-probe weak gravitational lensing and spectroscopic galaxy clustering constraints*, *Astron. Astrophys.* **646** (2021) A140 [arXiv:2007.15632] [INSPIRE].

[37] R. Dalal et al., *Hyper Suprime-Cam Year 3 results: Cosmology from cosmic shear power spectra*, *Phys. Rev. D* **108** (2023) 123519 [arXiv:2304.00701] [INSPIRE].

[38] S. Chen et al., *Analysis of DESI×DES using the Lagrangian effective theory of LSS*, *Phys. Rev. D* **110** (2024) 103518 [arXiv:2407.04795] [INSPIRE].

[39] J. Kim et al., *The Atacama Cosmology Telescope DR6 and DESI: structure formation over cosmic time with a measurement of the cross-correlation of CMB lensing and luminous red galaxies*, *JCAP* **12** (2024) 022 [arXiv:2407.04606] [INSPIRE].

[40] DES collaboration, *Dark energy survey year 3 results: cosmology from galaxy clustering and galaxy-galaxy lensing in harmonic space*, *Mon. Not. Roy. Astron. Soc.* **536** (2024) 1586 [arXiv:2406.12675] [INSPIRE].

[41] J. Harnois-Deraps et al., *KiDS-1000 and DES-Y1 combined: cosmology from peak count statistics*, *Mon. Not. Roy. Astron. Soc.* **534** (2024) 3305 [arXiv:2405.10312] [INSPIRE].

[42] A. Dvornik et al., *KiDS-1000: Combined halo-model cosmology constraints from galaxy abundance, galaxy clustering and galaxy-galaxy lensing*, *Astron. Astrophys.* **675** (2023) A189 [*Erratum ibid.* **688** (2024) C3] [arXiv:2210.03110] [INSPIRE].

[43] DES collaboration, *Dark Energy Survey Year 3 results: Cosmological constraints from galaxy clustering and weak lensing*, *Phys. Rev. D* **105** (2022) 023520 [arXiv:2105.13549] [INSPIRE].

[44] S. Kumar and R.C. Nunes, *Probing the interaction between dark matter and dark energy in the presence of massive neutrinos*, *Phys. Rev. D* **94** (2016) 123511 [arXiv:1608.02454] [INSPIRE].

[45] R. Murgia, S. Gariazzo and N. Fornengo, *Constraints on the Coupling between Dark Energy and Dark Matter from CMB data*, *JCAP* **04** (2016) 014 [arXiv:1602.01765] [INSPIRE].

[46] S. Kumar and R.C. Nunes, *Echo of interactions in the dark sector*, *Phys. Rev. D* **96** (2017) 103511 [arXiv:1702.02143] [INSPIRE].

[47] E. Di Valentino, A. Melchiorri and O. Mena, *Can interacting dark energy solve the H_0 tension?*, *Phys. Rev. D* **96** (2017) 043503 [arXiv:1704.08342] [INSPIRE].

[48] S. Bahamonde et al., *Dynamical systems applied to cosmology: dark energy and modified gravity*, *Phys. Rept.* **775-777** (2018) 1 [arXiv:1712.03107] [INSPIRE].

[49] S. Kumar, *Remedy of some cosmological tensions via effective phantom-like behavior of interacting vacuum energy*, *Phys. Dark Univ.* **33** (2021) 100862 [arXiv:2102.12902] [INSPIRE].

[50] S. Pan and W. Yang, *On the interacting dark energy scenarios — the case for Hubble constant tension*, arXiv:2310.07260 [DOI:10.1007/978-981-99-0177-7_29] [INSPIRE].

[51] D. Benisty et al., *Late-time constraints on interacting dark energy: Analysis independent of H0, rd, and MB*, *Astron. Astrophys.* **688** (2024) A156 [arXiv:2403.00056] [INSPIRE].

[52] W. Yang et al., *All-inclusive interacting dark sector cosmologies*, *Phys. Rev. D* **101** (2020) 083509 [arXiv:2001.10852] [INSPIRE].

[53] M. Forconi et al., *A double take on early and interacting dark energy from JWST*, *JCAP* **05** (2024) 097 [arXiv:2312.11074] [INSPIRE].

[54] A. Pourtsidou and T. Tram, *Reconciling CMB and structure growth measurements with dark energy interactions*, *Phys. Rev. D* **94** (2016) 043518 [arXiv:1604.04222] [INSPIRE].

[55] E. Di Valentino, *A combined analysis of the H_0 late time direct measurements and the impact on the Dark Energy sector*, *Mon. Not. Roy. Astron. Soc.* **502** (2021) 2065 [arXiv:2011.00246] [INSPIRE].

[56] E. Di Valentino and O. Mena, *A fake Interacting Dark Energy detection?*, *Mon. Not. Roy. Astron. Soc.* **500** (2020) L22 [arXiv:2009.12620] [INSPIRE].

[57] R.C. Nunes and E. Di Valentino, *Dark sector interaction and the supernova absolute magnitude tension*, *Phys. Rev. D* **104** (2021) 063529 [arXiv:2107.09151] [INSPIRE].

[58] W. Yang, A. Mukherjee, E. Di Valentino and S. Pan, *Interacting dark energy with time varying equation of state and the H_0 tension*, *Phys. Rev. D* **98** (2018) 123527 [arXiv:1809.06883] [INSPIRE].

[59] R. von Marttens et al., *Dark degeneracy I: Dynamical or interacting dark energy?*, *Phys. Dark Univ.* **28** (2020) 100490 [arXiv:1911.02618] [INSPIRE].

[60] M. Lucca and D.C. Hooper, *Shedding light on dark matter-dark energy interactions*, *Phys. Rev. D* **102** (2020) 123502 [arXiv:2002.06127] [INSPIRE].

[61] Y. Zhai et al., *A consistent view of interacting dark energy from multiple CMB probes*, *JCAP* **07** (2023) 032 [arXiv:2303.08201] [INSPIRE].

[62] A. Bernui et al., *Exploring the H0 tension and the evidence for dark sector interactions from 2D BAO measurements*, *Phys. Rev. D* **107** (2023) 103531 [arXiv:2301.06097] [INSPIRE].

[63] G.A. Hoerning et al., *Constraints on interacting dark energy revisited: Implications for the Hubble tension*, *Phys. Rev. D* **112** (2025) 023523 [arXiv:2308.05807] [INSPIRE].

JCAP11(2025)010

[64] W. Giarè et al., *Tightening the reins on nonminimal dark sector physics: Interacting dark energy with dynamical and nondynamical equation of state*, *Phys. Rev. D* **110** (2024) 063527 [arXiv:2404.02110] [INSPIRE].

[65] L.A. Escamilla, O. Akarsu, E. Di Valentino and J.A. Vazquez, *Model-independent reconstruction of the interacting dark energy kernel: Binned and Gaussian process*, *JCAP* **11** (2023) 051 [arXiv:2305.16290] [INSPIRE].

[66] M.A. van der Westhuizen and A. Abebe, *Interacting dark energy: clarifying the cosmological implications and viability conditions*, *JCAP* **01** (2024) 048 [arXiv:2302.11949] [INSPIRE].

[67] E. Silva, U. Zúñiga-Bolaño, R.C. Nunes and E. Di Valentino, *Non-linear matter power spectrum modeling in interacting dark energy cosmologies*, *Eur. Phys. J. C* **84** (2024) 1104 [arXiv:2403.19590] [INSPIRE].

[68] E. Di Valentino, A. Melchiorri, O. Mena and S. Vagnozzi, *Interacting dark energy in the early 2020s: A promising solution to the H_0 and cosmic shear tensions*, *Phys. Dark Univ.* **30** (2020) 100666 [arXiv:1908.04281] [INSPIRE].

[69] T.-N. Li et al., *Constraints on interacting dark energy models from the DESI BAO and DES supernovae data*, *Astrophys. J.* **976** (2024) 1 [arXiv:2407.14934] [INSPIRE].

[70] N.N. Pooya, *Growth of matter perturbations in the interacting dark energy-dark matter scenarios*, *Phys. Rev. D* **110** (2024) 043510 [arXiv:2407.03766] [INSPIRE].

[71] S. Halder, J. de Haro, T. Saha and S. Pan, *Phase space analysis of sign-shifting interacting dark energy models*, *Phys. Rev. D* **109** (2024) 083522 [arXiv:2403.01397] [INSPIRE].

[72] S. Castello et al., *Gravitational redshift constraints on the effective theory of interacting dark energy*, *JCAP* **05** (2024) 003 [arXiv:2311.14425] [INSPIRE].

[73] Y.-H. Yao and X.-H. Meng, *Can interacting dark energy with dynamical coupling resolve the Hubble tension*, *Phys. Dark Univ.* **39** (2023) 101165 [arXiv:2207.05955] [INSPIRE].

[74] K.R. Mishra, S.K.J. Pacif, R. Kumar and K. Bamba, *Cosmological implications of an interacting model of dark matter & dark energy*, *Phys. Dark Univ.* **40** (2023) 101211 [arXiv:2301.08743] [INSPIRE].

[75] R.C. Nunes, S. Pan and E.N. Saridakis, *New constraints on interacting dark energy from cosmic chronometers*, *Phys. Rev. D* **94** (2016) 023508 [arXiv:1605.01712] [INSPIRE].

[76] E.M. Teixeira et al., *Alleviating cosmological tensions with a hybrid dark sector*, arXiv:2412.14139 [INSPIRE].

[77] W. Giarè, M.A. Sabogal, R.C. Nunes and E. Di Valentino, *Interacting Dark Energy after DESI Baryon Acoustic Oscillation Measurements*, *Phys. Rev. Lett.* **133** (2024) 251003 [arXiv:2404.15232] [INSPIRE].

[78] C.G. Boehmer, G. Caldera-Cabral, R. Lazkoz and R. Maartens, *Dynamics of dark energy with a coupling to dark matter*, *Phys. Rev. D* **78** (2008) 023505 [arXiv:0801.1565] [INSPIRE].

[79] R.C. Nunes et al., *New tests of dark sector interactions from the full-shape galaxy power spectrum*, *Phys. Rev. D* **105** (2022) 123506 [arXiv:2203.08093] [INSPIRE].

[80] T. Josset, A. Perez and D. Sudarsky, *Dark Energy from Violation of Energy Conservation*, *Phys. Rev. Lett.* **118** (2017) 021102 [arXiv:1604.04183] [INSPIRE].

[81] A. Perez, D. Sudarsky and E. Wilson-Ewing, *Resolving the H_0 tension with diffusion*, *Gen. Rel. Grav.* **53** (2021) 7 [arXiv:2001.07536] [INSPIRE].

JCAP11(2025)010

[82] M. de Cesare and E. Wilson-Ewing, *Interacting dark sector from the trace-free Einstein equations: Cosmological perturbations with no instability*, Phys. Rev. D **106** (2022) 023527 [arXiv:2112.12701] [INSPIRE].

[83] J. Valiviita, E. Majerotto and R. Maartens, *Instability in interacting dark energy and dark matter fluids*, JCAP **07** (2008) 020 [arXiv:0804.0232] [INSPIRE].

[84] G.F.R. Ellis, H. van Elst, J. Murugan and J.-P. Uzan, *On the Trace-Free Einstein Equations as a Viable Alternative to General Relativity*, Class. Quant. Grav. **28** (2011) 225007 [arXiv:1008.1196] [INSPIRE].

[85] A. Perez and D. Sudarsky, *Dark energy from quantum gravity discreteness*, Phys. Rev. Lett. **122** (2019) 221302 [arXiv:1711.05183] [INSPIRE].

[86] A. Perez, D. Sudarsky and J.D. Bjorken, *A microscopic model for an emergent cosmological constant*, Int. J. Mod. Phys. D **27** (2018) 1846002 [arXiv:1804.07162] [INSPIRE].

[87] E. Albertini, A. Nasiri and E. Panella, *Stochastic dark matter: Covariant Brownian motion from Planckian discreteness*, Phys. Rev. D **111** (2025) 023514 [arXiv:2409.02188] [INSPIRE].

[88] S.J. Landau, M. Benetti, A. Perez and D. Sudarsky, *Cosmological constraints on unimodular gravity models with diffusion*, Phys. Rev. D **108** (2023) 043524 [arXiv:2211.07424] [INSPIRE].

[89] W. Hu, *Structure formation with generalized dark matter*, Astrophys. J. **506** (1998) 485 [astro-ph/9801234] [INSPIRE].

[90] M. Kopp, C. Skordis and D.B. Thomas, *Extensive investigation of the generalized dark matter model*, Phys. Rev. D **94** (2016) 043512 [arXiv:1605.00649] [INSPIRE].

[91] D.B. Thomas, M. Kopp and C. Skordis, *Constraining the Properties of Dark Matter with Observations of the Cosmic Microwave Background*, Astrophys. J. **830** (2016) 155 [arXiv:1601.05097] [INSPIRE].

[92] S. Ilić, M. Kopp, C. Skordis and D.B. Thomas, *Dark matter properties through cosmic history*, Phys. Rev. D **104** (2021) 043520 [arXiv:2004.09572] [INSPIRE].

[93] L. Amendola, *Coupled quintessence*, Phys. Rev. D **62** (2000) 043511 [astro-ph/9908023] [INSPIRE].

[94] C.-P. Ma and E. Bertschinger, *Cosmological perturbation theory in the synchronous and conformal Newtonian gauges*, Astrophys. J. **455** (1995) 7 [astro-ph/9506072] [INSPIRE].

[95] R. Percacci, *Unimodular quantum gravity and the cosmological constant*, Found. Phys. **48** (2018) 1364 [arXiv:1712.09903] [INSPIRE].

[96] S. Gielen, R. de León Ardón and R. Percacci, *Gravity with more or less gauging*, Class. Quant. Grav. **35** (2018) 195009 [arXiv:1805.11626] [INSPIRE].

[97] G.R. Bengochea, G. Leon, A. Perez and D. Sudarsky, *A clarification on prevailing misconceptions in unimodular gravity*, JCAP **11** (2023) 011 [arXiv:2308.07360] [INSPIRE].

[98] M. Henneaux and C. Teitelboim, *The Cosmological Constant and General Covariance*, Phys. Lett. B **222** (1989) 195 [INSPIRE].

[99] K.V. Kuchar, *Does an unspecified cosmological constant solve the problem of time in quantum gravity?*, Phys. Rev. D **43** (1991) 3332 [INSPIRE].

[100] J. Torrado and A. Lewis, *Cobaya: Code for Bayesian Analysis of hierarchical physical models*, JCAP **05** (2021) 057 [arXiv:2005.05290] [INSPIRE].

[101] J. Torrado and A. Lewis, *Cobaya: Bayesian analysis in cosmology*, Astrophysics Source Code Library, record ascl:1910.019, Oct., (2019).

[102] D. Blas, J. Lesgourgues and T. Tram, *The Cosmic Linear Anisotropy Solving System (CLASS) II: Approximation schemes*, *JCAP* **07** (2011) 034 [arXiv:1104.2933] [INSPIRE].

[103] Planck collaboration, *Planck 2018 results. I. Overview and the cosmological legacy of Planck*, *Astron. Astrophys.* **641** (2020) A1 [arXiv:1807.06205] [INSPIRE].

[104] Planck collaboration, *Planck 2018 results. V. CMB power spectra and likelihoods*, *Astron. Astrophys.* **641** (2020) A5 [arXiv:1907.12875] [INSPIRE].

[105] Planck collaboration, *Planck 2018 results. VIII. Gravitational lensing*, *Astron. Astrophys.* **641** (2020) A8 [arXiv:1807.06210] [INSPIRE].

[106] DESI collaboration, *DESI 2024 III: baryon acoustic oscillations from galaxies and quasars*, *JCAP* **04** (2025) 012 [arXiv:2404.03000] [INSPIRE].

[107] DESI collaboration, *DESI 2024 IV: Baryon Acoustic Oscillations from the Lyman alpha forest*, *JCAP* **01** (2025) 124 [arXiv:2404.03001] [INSPIRE].

[108] DESI collaboration, *DESI 2024 VI: cosmological constraints from the measurements of baryon acoustic oscillations*, *JCAP* **02** (2025) 021 [arXiv:2404.03002] [INSPIRE].

[109] D. Brout et al., *The Pantheon+ Analysis: Cosmological Constraints*, *Astrophys. J.* **938** (2022) 110 [arXiv:2202.04077] [INSPIRE].

[110] A. Lewis, *Efficient sampling of fast and slow cosmological parameters*, *Phys. Rev. D* **87** (2013) 103529 [arXiv:1304.4473] [INSPIRE].

[111] Planck collaboration, *Planck intermediate results. LVII. Joint Planck LFI and HFI data processing*, *Astron. Astrophys.* **643** (2020) A42 [arXiv:2007.04997] [INSPIRE].

[112] J. Carron, M. Mirmelstein and A. Lewis, *CMB lensing from Planck PR4 maps*, *JCAP* **09** (2022) 039 [arXiv:2206.07773] [INSPIRE].

[113] G. Efstathiou and S. Gratton, *A Detailed Description of the CamSpec Likelihood Pipeline and a Reanalysis of the Planck High Frequency Maps*, arXiv:1910.00483 [DOI:10.21105/astro.1910.00483] [INSPIRE].

[114] DESI collaboration, *DESI 2024 VII: cosmological constraints from the full-shape modeling of clustering measurements*, *JCAP* **07** (2025) 028 [arXiv:2411.12022] [INSPIRE].

[115] M.A. Sabogal et al., *Quantifying the S8 tension and evidence for interacting dark energy from redshift-space distortion measurements*, *Phys. Rev. D* **110** (2024) 123508 [arXiv:2408.12403] [INSPIRE].

[116] S. Pan, W. Yang, C. Singha and E.N. Saridakis, *Observational constraints on sign-changeable interaction models and alleviation of the H_0 tension*, *Phys. Rev. D* **100** (2019) 083539 [arXiv:1903.10969] [INSPIRE].

[117] D. Benisty, D. Vasak, J. Kirsch and J. Struckmeier, *Low-redshift constraints on covariant canonical Gauge theory of gravity*, *Eur. Phys. J. C* **81** (2021) 125 [arXiv:2101.07566] [INSPIRE].

[118] A.J. Shajib and J.A. Frieman, *Scalar-field dark energy models: Current and forecast constraints*, *Phys. Rev. D* **112** (2025) 063508 [arXiv:2502.06929] [INSPIRE].

[119] W. Yang et al., *2021-H0 odyssey: closed, phantom and interacting dark energy cosmologies*, *JCAP* **10** (2021) 008 [arXiv:2101.03129] [INSPIRE].